

# DETC00/MECH-14115

## EXPERIMENTS IN THE COMMUTATION AND MOTION PLANNING OF A SPHERICAL STEPPER MOTOR

**David Stein, Graduate Student**

Robotics and Electro-Mechanical Systems Laboratory  
Department of Mechanical Engineering  
The Johns Hopkins University  
Baltimore, Maryland 21218  
email: brawler@jhu.edu

**Gregory S. Chirikjian,<sup>1</sup> Associate Professor**

Robotics and Electro-Mechanical Systems Laboratory  
Department of Mechanical Engineering  
The Johns Hopkins University  
Baltimore, Maryland 21218  
email: gregc@jhu.edu

### **ABSTRACT**

*This paper addresses the commutation and motion planning of a spherical stepper motor in which the poles of the stator are electromagnets and the poles of the rotor (rotating ball) are permanent magnets. The stator only overlaps a very small area of the rotor, leading to a design that has a much wider range of unhindered motion than other spherical stepper motors in the literature. The problem with having a small stator is that it makes commutation and motion planning a difficult problem. We first explore the techniques and model used to construct the proper sequence of stator activations that result in the desired rotor trajectory. Experimental results are then presented for the model and prototype we have constructed.*

### **1 INTRODUCTION**

This paper addresses experimental aspects of the commutation and motion planning of spherical stepper motors with a large range of motion. The work presented here builds on the previous work we have done on this topic [1]. Our previous work presents some of the mathematical techniques used in the design of this type of motor.

Potential applications of spherical motors are numerous. They include: (1) robotic wrist, elbow, and shoulder actuators (allowing six or nine degrees of freedom to be designed compactly into a small space); (2) camera actuators for computer vision [2]; (3) omnidirectional wheels for mobile robots; (4) actuator arrays capable of transporting

objects in any direction [3, 4]; and (5) attitude control mechanisms for spacecraft. See Figure 1 illustrations of some of these applications.

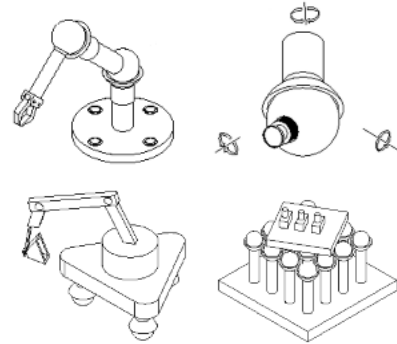


Figure 1: APPLICATIONS OF SPHERICAL MOTORS

#### **1.1 Previous Work**

The concept of a spherical motor is not new. Our work builds on the accomplishments of a number of notable works. The basic operating principles of spherical DC induction motors have been known for quite some time, see e.g. [5, 6]. Kaneko et al [7] developed a spherical DC servo motor. The design and implementation of spherical variable-reluctance motors has been studied by Kok-Meng Lee and coworkers for a number of years [8, 9, 10, 11]. Toyama and coworkers have developed spherical ultrasonic

---

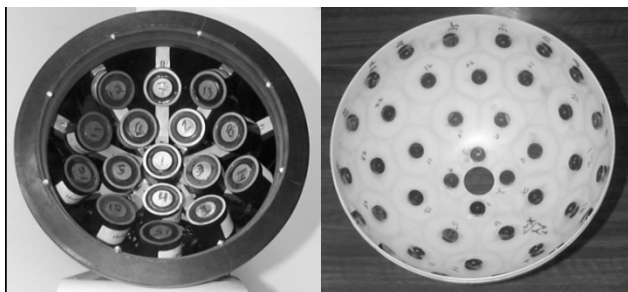
<sup>1</sup>Address all correspondence to this author.

motors [12, 13]. In the literature, one even finds actuators with a full six degrees of freedom, e.g. [14].

## 1.2 Our Prototype

The implementation of our spherical stepper motor was achieved by placing cylindrical rare-earth permanent magnets along the inside surface of a hollow plastic sphere (with magnetic poles aligned with axes of the sphere) to form the rotor. The stator consists of off-the-shelf wrapped soft iron cores placed on the outside of a spherical cap which are polarized to form electromagnetic fields. Due to the fact that the symmetry of the rotor pole arrangement is different than that of the stator poles, the fields created by energizing stator coils provide a torque that changes the orientation of the rotor. A key feature of our design that is different than others found in the literature is that the stator does not envelop the rotor. In fact, it covers less than a hemisphere. As a result, our design is able to achieve a much wider range of motion.

A 12 inch diameter plastic sphere is used as the rotor. The rotor was assembled by fixing permanent magnets, .75 inches in diameter to the inside of the sphere. The sphere is very rigid and splits into two pieces making it easy to alter the packing of the permanent magnets. It is crucial that the magnets be positioned with high accuracy. The ball should have no internal torques. For this to be possible the principal moments of inertia of the rotor have to be equal ( $I_{xx} = I_{yy} = I_{zz}$ ). If semi-regular packing are used[1], then the rotor in theory is balanced, however if the magnets are not positioned accurately a heavy region will develop resulting in an internal torque. A tapered pedestal acts as the base, houses the stator structure, and supports the rotor.



Stator                      Rotor  
Figure 2: STATOR AND ROTOR PACKINGS

An adjustable magnet saddle holds the stator magnets. The saddle serves two functions. It positions and orients the stator magnets and provides internal structure for the pedestal. By making different saddles, the stator packing

can be changed. The saddle can slide up and down in the pedestal to adjust the reluctance of the rotor. The stator electromagnets chosen are 2" diameter by 1.625" high. The individual semi-regular packing used for the rotor and stator are shown installed on the prototype in Figure 2.

A ring housing machined out of garolite and eight miniature ball-casters support the rotor. The ring is press fit into the top of the motor pedestal and positions the castors to be perpendicular to the ball at the contact points. This ring levitates the rotor above the stator magnets and allows the rotor to move relatively friction free. Five removable posts with ball castors at the terminal ends are also used to support the rotor from inside the stator assembly. PC relay boards control the states of the stator electromagnets. Power for the electromagnets is supplied by a standard 24 volt magnet supply rated up to a 100 watts of power. The final assembly is shown in Figure 3.

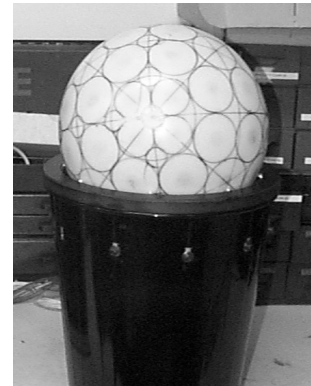


Figure 3: COMPLETE MOTOR ASSEMBLY

## 2 ROTOR-STATOR CONFIGURATIONS

Central to the design of spherical motors is the selection of compatible rotor and stator geometries. In the same way that standard cylindrical motors must not have the same number of rotor and stator poles in order to operate, the symmetries of spherical rotors and stators must not be the same. The question then becomes one of finding which combination of stator and rotor arrangements is the most appropriate. Since there is a very limited number of regular arrangements of points on the sphere (there are only five corresponding to the Platonic solids), and since these are far too coarsely distributed for use in a discrete-state motor capable of the applications discussed earlier, the question becomes one of finding compatible semi-regular rotor and stator arrangements.

## 2.1 Packings Used in Prototype

As a rule, semi-regular packings do not possess the degree of symmetry that the regular packings do. This is quite important in the context of a spherical stepper, where the rotor and stator poles must have some compatibility in order to be able to commutate. The most critical similarity that rotor/stator packings must share are compatible “center lengths.” These center lengths can be looked at as the angular distance between the centers of two magnets on the surface of the sphere. Compatible rotor/stator packings must share many different center lengths. These center lengths do not have to be identical, but must be within a certain error. This error is a function of the magnet combination being used. It is desirable that this error be small enough that the center of the rotor magnets is still within the peak magnetic attraction of the stator magnet.

Our rotor uses a semi-regular packing based on octahedral symmetry, while the stator uses a semi-regular packing based on icosahedral symmetry as shown in Figure 2. They were chosen because they share many center lengths. This is the only rotor/stator combination we have conducted experiments with, but the flexibility of our prototype allows us to conduct further experiments in the future with different combinations.

## 3 COMMUTATION AND MOTION PLANNING

In this section, the model we use for the commutation and motion planning will be discussed. The model is geometric in nature, but uses the idea of a potential function presented in section 3 of [1]. The model will be explained step by step, highlighting its features and limitations.

Before a model can be built, the operational characteristics of a spherical stepper motor have to be reviewed. Like a standard stepper motor, the spherical stepper motor will “step” between stable configurations. The rotor in the spherical case is fixed by two or more rotor/stator pairs. Two active rotor/stator pairs are always needed to hold the ball in a stable configuration. The explanation for this is that one rotor/stator pair fixes the rotor so it can only rotate about this attraction point. The other rotor/stator pair constrains this rotation, resulting in a fully constrained rotor. To produce motion of the rotor, a commutation model has been developed. It is used to find the next rotor/stator pairs to be activated, stepping the motor to another stable state, resulting in the desired motion. This commutation model has been developed to use two rotor/stator pairs to fix the rotor, but Section 3.2 describes a model expanded to three or more rotor/stator pairs. Before we can explain the model we have to review some mathematical preliminaries.

## 3.1 Mathematical Preliminaries

The properties of the vector dot product are used extensively in this model. Recall that the dot product of two vectors  $\bar{a}$  and  $\bar{b}$  is the product of their lengths times the cosines of their angle  $\theta$ .

$$\bar{a} \cdot \bar{b} = \|\bar{a}\| \|\bar{b}\| \cos(\theta)$$

Positions on the unit sphere,  $S^2$ , are parametrized using spherical coordinates:

$$\bar{u}(\phi, \theta) = \begin{pmatrix} \cos \phi \sin \theta \\ \sin \phi \sin \theta \\ \cos \theta \end{pmatrix}.$$

$\theta$  and  $\phi$  are called the polar and azimuthal angles, respectively.

The distance between two points  $\bar{r}, \bar{s} \in S^2$  as measured along the shorter segment of the great arc connecting the points is calculated as

$$d(\bar{r}, \bar{s}) = \cos^{-1}(\bar{r} \cdot \bar{s})$$

where in the context of the current discussion  $\cos^{-1}(\cdot)$  takes values in the range  $[0, \pi]$ . In this way the length of the shorter of the two great arcs connecting  $\bar{r}$  and  $\bar{s}$  is automatically chosen.

The concept of rigid body rotations is another important concept used in this model. Motion of the rotor in this model is viewed as the rotation of unit vectors locating magnetic centers on the surface of the rotor sphere. A general rotation is written as

$$R = \text{ROT}[\bar{n}, \theta] = \exp[\theta N]$$

$$= 1_{3 \times 3} + \sin \theta N + (1 - \cos \theta) N^2 = Q_i \text{ROT}[\bar{e}_i, \theta] Q_i^T$$

where  $N$  is the skew symmetric matrix satisfying  $N\bar{x} = \bar{n} \times \bar{x}$  for all  $\bar{x} \in \mathbb{R}^3$ ,  $\bar{n} = \text{vect}(N)$  is the unit vector specifying the axis of rotation, and  $\theta$  is the angle of rotation.  $1_{3 \times 3}$  is the  $3 \times 3$  identity matrix. The rotations about the natural basis vectors  $\bar{e}_i$  are denoted  $\text{ROT}[\bar{e}_i, \theta]$ , and  $Q_i$  is any rotation matrix whose  $i^{th}$  column is the vector  $\bar{n}$ . The functions [15]

$$\theta(R) = \cos^{-1} \left( \frac{\text{tr}(R) - 1}{2} \right)$$

and

$$\bar{n}(R) = \frac{1}{2 \sin \theta(R)} \text{vect}(R - R^T)$$

can be thought of as those which extract the angle  $\theta$  and axis  $\bar{n}$  from the rotation matrix  $R = \text{ROT}[\bar{n}, \theta]$ .

### 3.2 Commutation Model

The commutation model we have developed is very flexible and can be used for any rotor/stator packing pair. The model requires the following inputs: the rotor/stator packing, the desired rotation axis, and the desired angle of rotation about this axis. Some other variables are experimentally determined, or are used to “tune” the model. They will be explained as they come up in the explanation of the model. The commutation model starts with an initial orientation. The highly symmetric nature of the rotor/stator packings enables us to use any initial orientation. If the rotor and stator were constructed by packings of low symmetry, then the initial commutation would have a large effect on future motions of the rotor.

The first step of the model is to calculate the distance along the sphere between all the stator magnets and the rotor magnets located in the bottom hemisphere of the rotor at the present commutation state. We set a maximum distance of magnet attraction. This distance was derived experimentally by measuring the maximum distance over which the rotor/stator pairs exhibit an adequate attraction. An array with dimensions equal to the number of stator magnets by number of rotor magnets is constructed. The  $ij^{th}$  entry of this array corresponds to the measure distance between the  $i^{th}$  stator electromagnet and the  $j^{th}$  rotor pole. If the distance is greater than the maximum distance defined, a zero is placed in that entry. We now have an array of all the possible commutation pairs.

The commutation pairs now have to be sorted to extract the combination that will produce the desired torque on the rotor. Figure 4 is a flowchart that illustrates the computation steps involved in determining the acceptable rotor/stator pairs. Step one checks whether the torque produced by the attraction of the candidate rotor/stator pair will be about the desired rotation axis. The second step assures that the line of the attraction vector is approximately perpendicular to the imaginary torque arm. If there are no candidate pairs left after step 1 and 2, step 3 increase the error bounds and repeats the process. The variables in the flow chart are the following:  $\bar{n}$  is the desired rotation axis,  $\bar{r}$  is the unit vector locating the rotor magnet under evaluation,  $\bar{s}$  is the unit vector locating the stator electromagnet

under evaluation, and the error value starts at  $\pi/24$ .

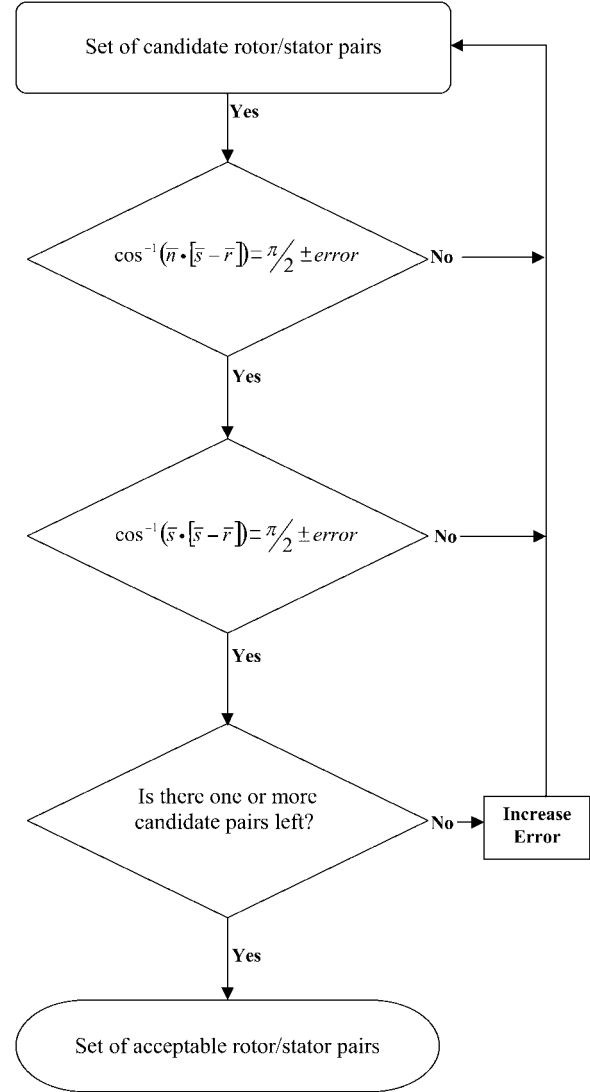


Figure 4: ACCEPTABLE ROTOR/STATOR PAIRS

We now have a list of rotor/stator pairs that will produce the proper torque about the desired rotation axis within some bounds. Since the rotor in its current commutation is being fixed by two stator magnets, we have to choose one pair as the stationary point. Using one of the stator magnets as the stationary point, the motion caused by each individual candidate pair is now calculated. This is repeated for the other stator magnet. A potential field model is used to find the stable state the rotor will assume after the stepping of rotor/stator pairs. The basis of the model used is discussed in section 3.2 of [1]. When we eval-

uate each candidate, the magnitude of rotor rotation about the desired rotation axis, and the error between the desired and actual rotation axes are recorded for each pair. Any pairs that produce large axis errors are discarded to leave two lists of applicable pairs.

From the resulting list there is a large number of possible paths that the rotor can follow from the initial commutation state to the desired state. If each step has three candidate rotor/stator pairs, and five steps are performed, the resulting number of possible paths is  $3^5 = 243$ . Since it is not efficient to evaluate all the possible paths, decisions have to be made at each step. Three basic schemes can be used: one that minimizes axis error, one that maximizes rotation angle, and one that weights both the rotation angle and axis error to make a choice. The choice of which scheme to use depends on the application and adds another layer of flexibility to the model. When a candidate pair is chosen the rotor is rotated into its potential state and the model is run again until the desired rotation angle is achieved.

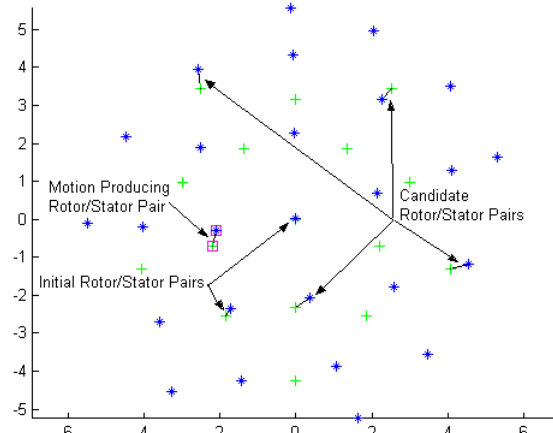


Figure 5: INITIAL COMMUTATION STATE

### 3.3 Model Output

The output of the model is a data file and a graphical representation of the commutation. The data file can be used two ways. The first is pseudo-realtime, where the rotor/stator pairs are switched as the model chooses them. The second method is to load the data file and step through the predicted motion.

The graphical output is very useful in gaining an understanding of commutation dynamics. Figure 5 is the graphical output of the model. The output is for an initial commutation state. In the figure, the '+' are the centers of stator magnets, and the '\*' are the centers of rotor magnets that

lie on the surface of a sphere projected onto the X-Y plane. Only rotor magnets that are applicable to the model at the present state are shown. The rotor and stator magnets that are connected by a line represent the candidate rotor/stator pairs. The rotor/stator pairs that the model chose are highlighted by the boxes that are drawn around them. Figure 6 shows a 3-D view of the model output. In this view the representation of the actual and desired rotation axes can be seen. These 3-D figures are also useful because they can be rotated into different view, giving greater insight into the commutation of the motor.

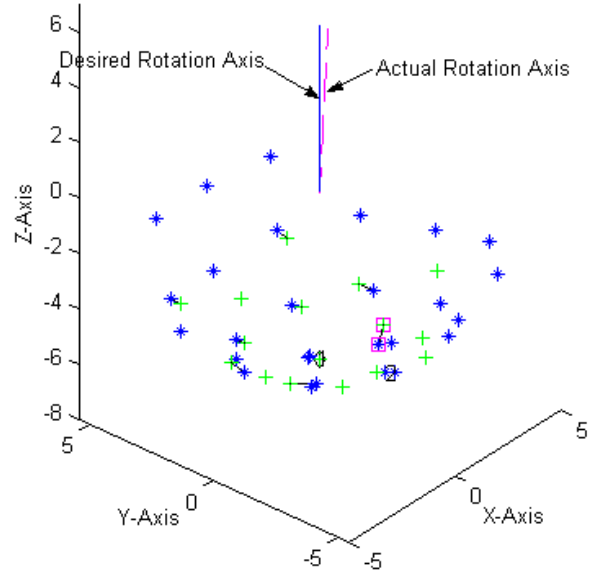


Figure 6: MODEL OUTPUT

### 3.4 Alternate Technique

The most efficient way to increase holding and switching torque on the rotor is to use more than two rotor/stator pairs. A commutation model that selects more than two candidate rotor/stator pairs would use the same basic technique outlined earlier. The difference lies in determining the equilibrium state the rotor will assume when held by the three or more rotor/stator pairs.

To find the equilibrium state of the rotor when fixed by three or more rotor/stator pairs we propose the use of a 'Dynamic' technique. This technique starts by selecting a method to describe the orientation of the rotor. Euler angles have the minimal dimension for this task, but have some unpleasant analytical properties at some orientations. Quaternion representation is free of singularities and is a

good chose[16].

The quaternion is defined  $\bar{q}$  as the  $4 \times 1$  matrix

$$\bar{q} = \begin{bmatrix} q_1 \\ q_2 \\ q_3 \\ q_4 \end{bmatrix} = \begin{bmatrix} \mathbf{q} \\ q_4 \end{bmatrix}$$

where,

$$\mathbf{q} = \begin{bmatrix} q_1 \\ q_2 \\ q_3 \end{bmatrix} = \sin(\phi/2) \hat{a}, \quad q_4 = \cos(\phi/2)$$

The unit vector  $\hat{a}$  is the rotation axis, and  $\phi$  is the rotation angle. The quaternion has one more component than it needs, so a constraint is placed on the elements:

$$q_1^2 + q_2^2 + q_3^2 + q_4^2 = 1$$

Using quaternion representation, the equations of motion for a rigid body subject to torques, with  $\omega$  as the angular velocity can be written as:

$$\frac{d}{dt} \mathbf{q} = \frac{1}{2} (q_4 \boldsymbol{\omega} - \boldsymbol{\omega} \times \mathbf{q})$$

$$\frac{d}{dt} q_4 = -\frac{1}{2} \boldsymbol{\omega} \cdot \mathbf{q}$$

$$\frac{d}{dt} \boldsymbol{\omega} = I_B^{-1} [-\boldsymbol{\omega} \times (I_B \boldsymbol{\omega}) + \mathbf{N}_B(\bar{q})]$$

The interaction between the rotor/stator pairs result in a torque being applied to the rotor. The magnitude and direction of this torque is a function of the orientation of the rotor. The sum of all the candidate rotor/stator torques make up the forcing of the system, showing up in the equations of motion as  $\mathbf{N}_B(\bar{q})$ . The rotor's principal moments of inertia are equal, resulting in a  $I_B$  which is a scaled identity matrix.

The equilibrium state of the rotor can now be found by constructing the forcing vector  $\mathbf{N}_B(\bar{q})$  which depends on the candidate rotor/stator pairs under evaluation. Damping is added to the system and the differential equations are solved numerically to determine the equilibrium state the rotor will assume. The orientation the rotor settles into is the equilibrium state for the candidate rotor/stator pairs.

## 4 EXPERIMENTAL RESULTS

The experimental results are broken down into two sections. The first is the results from the model that show discretized motion is possible for all rotation axes. The second is how well this motion is realized on our prototype.

### 4.1 Model Results

Results obtained from the model are path dependent. The results presented were obtained using a simple path choosing algorithm. This algorithm subtracts the axis error from the rotation angle and the candidate pair with the largest resulting value is chosen. Figure 7 is a plot of axis error vs. rotation angle for rotation about the Z axis. The Z axis is the extension of the symmetry axis of the base with its origin at the center of the rotor. The plot illustrates that over 90 degrees of rotor motion, the axis error is never greater than three degrees. This high resolution is possible because there is a stator magnet on the rotation axis. This rotor/stator pair becomes the rotation axis during the rotor motion. This very high resolution is possible for all rotation axes passing through or between stator poles.

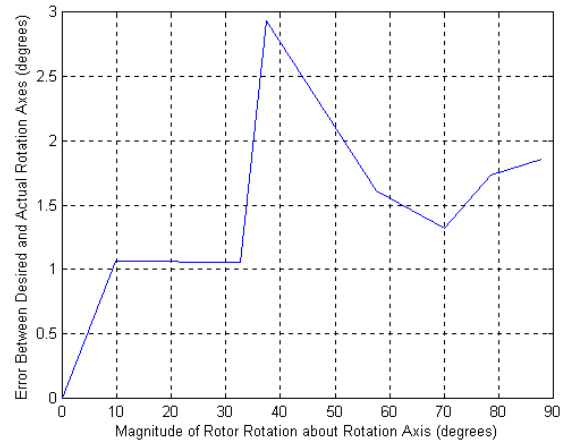


Figure 7: AXIS ERROR VS. ROTATION ANGLE (Z AXIS)

Using the present commutation model the resolution decreases as the rotor rotation axis gets farther away from the stator envelope. This is caused by the constraint that the rotor must always rotate about a stator magnet. This causes the actual rotation axis to be located in a conical region about the desired rotation axis. The rotation axes with the highest axis error are the axes that lie on the X-Y plane. Figure 8 is a plot of axis error vs. rotation angle for rotation about the Y axis. The model predicts that even under the most difficult circumstances the axis error is never more than 15 degrees.

### 4.2 Prototype Performance

We have had mixed results from the prototype. The prototype can reliably perform rotor motion if the span of the rotation axis is contained in the stator. Problems arise when the rotation point switches during each step. These problems arise from the characteristic of the stator electromagnets. In practice the stator electromagnets have a

relatively broad potential well, instead of a desirable sharp minimum. This broad well produces “slop” in the rotor in a stable commutation state. The error caused by this “slop” builds during each step and kills the predictability of the rotor state. Carefully choosing the commutation path lessens this effect, but also greatly cuts down on the predicted performance. To solve this problem we are planning to substitute stator magnets custom wound to our specifications, instead of relying on inexpensive, off-the-shelf components.

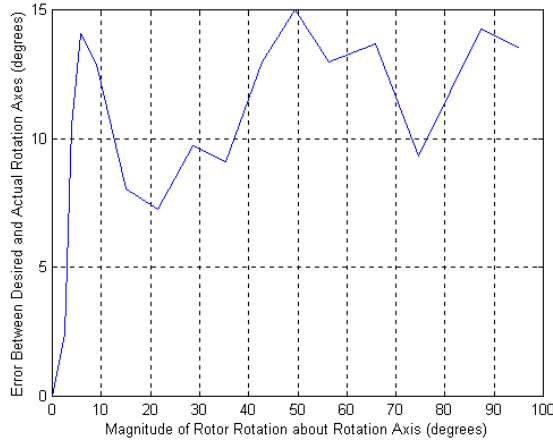


Figure 8: AXIS ERROR VS. ROTATION ANGLE (Y AXIS)

## 5 SUMMARY AND CONCLUSIONS

We have developed a theory for the commutation and motion planning of spherical stepper motors where the rotor consists of permanent magnets. Experiments performed on the prototype prove the theories and techniques presented in this paper. Many options for improvement have been given in a framework flexible enough for many motor geometries. Much of our future work will be in further development of our prototype and expansion of our model.

## Acknowledgments

This work was performed under NSF grant IIS-9731720 from the Robotics and Human Augmentation Program. We thank Ms. Yunfeng Wang for creating the drawings in Figure 1.

## REFERENCES

- Chirikjian, G.S., Stein, D., "Kinematic Design and Commutation of a Spherical Stepper Motor," *IEEE/ASME Transactions on Mechatronics*, Vol. 4, No. 4, December 1999, pp.342-353
- Bederson, B.B., Wallace, R.S., Schwartz, E.L., "A Miniature Pan-Tilt Actuator: The Spherical Pointing Mo-

tor," *IEEE Trans. on Robotics and Automation*, Vol. 10, No. 3, June 1994, pp. 298-308.

Donald, B.R., Jennings, J., Rus, D., "Information Invariants for Distributed Manipulation," *International Journal of Robotics Research* v. 16 n. 5 Oct 1997, pp. 673-702.

Luntz, J., Messner, W., Choset, H., "Parcel Manipulation and Dynamics with a Distributed Actuator Array: The Virtual Vehicle," *Proc. 1997 IEEE International Conference on Robotics and Automation*, 1997.

Williams, F., Laithwaite, Eastham, G.F., "Development and Design of Spherical Induction Motors," *Proc. of the IEEE*, pp. 471-484, Dec. 1959.

K. Davey, G. Vachtsevanos, "The Analysis of Fields and Torques in a Spherical Induction Motor," *IEEE Trans. Magn.*, vol. MAG-23, Mar. 1987.

Kaneko, Y., Yamada, I., Itao, K., A Spherical DC Servo Motor with Three Degrees-of-Freedom," *ASME Dynamic Systems and Controls Division*, Vol. 11, pp. 398-402, 1988.

Lee, K.-M., Kwan, C.-K., "Design Concept Development of a Spherical Stepper for Robotic Applications, *IEEE Trans. on Robotics and Automation*, Vol. 7, No. 1, Feb. 1991, pp. 175-181.

Roth, R.B., Lee, K.-M., "Design Optimization of a Three Degrees-of-Freedom Variable-Reluctance Spherical Wrist Motor," *ASME J. Engineering for Industry*, Vol. 117, August 1995, pp. 378-388.

Zhou, Z., Lee, K.-M., "Real-time Motion Control of a Multi-degree-of-freedom Variable Reluctance Spherical Motor," *Proc. 1996 IEEE Int. Conf. on Robotics and Automation*, Minneapolis, Minnesota, April 1996, pp. 2859-2864.

Pei, J., "Methodology of Design and Analysis of Variable-Reluctance Spherical Motors," Ph.D Dissertation, Dept. of Mechanical Engineering, Georgia Inst. of Technology, 1990.

Toyama, S., Sugitani, S., Zhang, G., Miyatani, Y., Nakamura, K., "Multi degree of freedom Spherical Ultrasonic Motor," *Proc. 1995 IEEE Int. Conf. on Robotics and Automation*, Nagoya, Japan, pp. 2935-2940.

Toyama, S., Zhang, G., Miyoshi, O., "Development of New Generation Spherical Ultrasonic Motor," *Proc. 1996 IEEE Int. Conf. on Robotics and Automation*, Minneapolis, Minnesota, April 1996, pp. 2871-2876.

Hollis, R.L., Salcudean, S.E., Allan, A.P., "A Six-Degree-of-Freedom Magnetically Levitated Variable Compliance Fine-Motion Wrist: Design, Modeling, Control," *IEEE Trans. Rob. and Aut.* Vol. 7, No. 1, pp. 320-332, June 1991.

McCarthy, J.M., *Introduction to Theoretical Kinematics*, MIT Press, 1990.

Pisacane, V.L., Moore, R.C., *Fundamentals of Space Systems*, Oxford University Press, 1994